Available online at www.sciencedirect.com
SCIENCE DIRECT
Polymer 47 (2006) 5467–5477
polymer
www.elsevier.com/locate/polymer

Morphology and crystal structures of poly(2,6-naphthalene terephthalate) and poly(2,6-naphthalene naphthalate)☆

Jinfeng Wang [a], Phillip H. Geil [a,*], Martina Kaszonyiova [b], Frantisek Rybnikar [b]

[a] *Department of Materials Science and Engineering, University of Illinois, 1304 W. Green Street, Urbana, IL 61801, USA*
[b] *Tomas Bata University of Zlin, Zlin, Czech Republic*

Received 10 February 2005; accepted 20 February 2005
Available online 19 May 2006

Abstract

The morphology and crystal structures of poly(2,6-naphthalene terephthalate) (PNT) and poly(2,6-naphthalene naphthalate) (PNN), prepared by confined thin film melt/solution polymerization (CTFMP/CTFSP), were characterized by transmission electron microscopy, electron diffraction and molecular modeling. The unit cells of PNT and PNN are both monoclinic ($P12_1/a1$ space group) with parameters $a=8.18$ Å, $b=5.80$ Å, $c=14.9$ Å and $\beta=101.9°$ for PNT, and $a=7.85$ Å, $b=5.97$ Å, $c=17.1$ Å and $\beta=99.5$ for PNN, respectively. Simulated ED patterns from the proposed unit cells agree well with the observed ED patterns. The crystal structures of PNT and PNN are also compared with those of poly (*p*-phenylene naphthalate) (PPN) and poly(2,6-oxynaphtalate) (PONA).

Keywords: Poly(2,6-naphthalene terephthalate); Poly(2,6-naphthalene naphthalate); Electron diffraction

1. Introduction

In recent years aromatic polyesters have been accepted as high performance polymers due to their excellent thermal and mechanical properties. In our lab electron diffraction (ED) has been used to investigate the crystal structure of a series of aromatic polyesters. Crystals prepared by confined thin film polymerization techniques generally consist of extended chain lamellae ca. 100 Å thick, yielding [001] zone with *hk*0 spacings. Methods for obtaining zones containing *hkl* reflections were developed, including specimen tilting, polymer shearing and epitaxial growth between mica. A series of polyesters have been studied using the above techniques [1–13], including characterization of the crystal structure of poly(2,6-oxynaphthoate) (PONA) [8,15] and recently published results on poly(*p*-phenylene terephthalate) (PPT) [12] and poly(phenylene 2,6-naphthalate) (PPN) [13]. In this paper, we report our recent results on determination of the crystal structure of poly(2,6-naphthalene terephthalate) (PNT), a polymer similar to PPN in chemical structure with the ester groups reversed, and poly(2,6-naphthalene 2,6-naphthalate) (PNN), which is a symmetric version of PONA. To our knowledge, it is the first report on the crystal structure determinations of PNT and PNN.

2. Experimental

2.1. Materials

2,6-Dihydroxynaphthalene (2,6-DHN, 98%, Research Chemicals Ltd, $F_w=160.17$, $M_p=223$–225 °C), 2,6-diacetoxynaphthalene (2,6-DAN, 99%, Tokyo Kasei Kogyo Co. Ltd, $F_w=244.24$, $M_p=177$ °C), 2,6-naphthalenedicarboxylic acid dimethyl ester (2,6-NDADME, Tokyo Kasei, $F_w=244.25$, $M_p=187$ °C), and terephthaloyl chloride (TCI, 99+%, Acros Organics, $F_w=203.02$, $M_p=180$ °C) were used as provided. High purity acetone (Optima, Fisher Scientific) was used to minimize the residue after evaporation. Therminol® 66 (Solutia, Inc.) and Marlotherm® SH (Creanova, Inc.), heat transfer fluids, were used as high temperature solvents without any treatment. 2% HF was diluted from 49% hydrofluoric acid (Fisher Scientific). Glass cover slips (Corning cover glass) and freshly cleaved mica were used as substrates for the polymerization.

☆ Dedicated to Prof D. Bassett on the occasion of his retirement

* Corresponding author. Tel.: +1 217 333 0149; fax: +1 217 333 2736.
E-mail address: geil@uiuc.edu (P.H. Geil).

0032-3861/$ - see front matter © 2006 Elsevier Ltd. All rights reserved.
doi:10.1016/j.polymer.2005.02.131

2.2. Confined thin film melt polymerization (CTFMP), confined thin film solution polymerization (CTFSP), and bulk polymerization

The CTFMP of PNT was carried out as previously described [14], 1% (wt/v) acetone solution of the mixed monomers (TC + 2,6-DHN unless otherwise specified) in 1:1 mole ratio being cast on glass cover slips or mica, covered with the same substrate and heated on a thermostatted hot plate at various temperatures for various time (described by temperature (°C) / time (hours) in the rest of the paper).

For CTFMP of PNN, since 2,6-NDADME is insoluble in acetone, powders of mixed monomers in 1:1 molar ratio were polymerized between glass cover slips or mica on a hot plate at 250 °C for 18 h under nitrogen gas.

The CTFSP samples were prepared by confining Therminol® 66 or Marlotherm® SH solutions (1–4%) of the mixed monomers between mica or glass substrates, placing a stack of such substrates with monomer solutions in between in the same solution and polymerizing at relatively high temperatures (300 °C).

In order to prepare sufficient material for X-ray diffraction, FTIR and solid state NMR measurements, PNT powder samples were also obtained by solution and bulk melt polymerization.

2.3. TEM and electron diffraction

After polymerization (CTFMP or CTFSP), the two substrates with the polymers on the inner surfaces were separated, washed with acetone to remove residual monomers and low molecular weight oligomers, and then, in a vacuum chamber, reinforced with a thin layer of carbon and shadowed with Pt/C for imaging or decorated with gold for ED in-situ calibration. The sample was removed from the substrate by floating on a 2% HF solution, picked up by a copper grid and inserted into a Philips CM12 (S)TEM for observation after drying.

The ED patterns were scanned with a Microtek ArtixScan 1800f scanner and ScanWizard Pro 7 software (gray scale, positive mode) at 600 dpi. The spacings were measured with Image J 1.29× software (National Institute of Health, USA). A least square refinement program was used for determination of the cell parameters. (Program courtesy of Zhang, University of Akron)

2.4. Molecular simulation

The molecular simulation program Cerius^2 (Accelrys Inc., San Diego, CA, version 4.9) with the Drieding force field was used, as previously described [3], to simulate the molecular conformation and packing in the unit cell and the resultant electron diffraction patterns.

The intramolecular interactions utilized (valence terms) include bond stretching, angle bending, torsional and inversion terms. The intermolecular interactions include van der Waals and Coulombic terms. For our periodic system the Ewald summation method was used in the minimizing calculations. Van der Waals interactions between atoms separated by three bonds were excluded from the energy term. A minimized chemical repeat unit of a single molecule was used to build the unit cell with selected space group symmetry. For the simulated ED patterns, torsion angle, crystal thickness and intensity factor were varied to obtain best agreement between the simulated and observed patterns. No rigid angular rotation, which was used for many polymers studied previously, was needed for the unit cell of PNT and PNN.

2.5. WAXS, solid-state ^{13}C NMR and FTIR

WAXS powder patterns were obtained with a Bruker general area detector diffraction system (GADDS) using Cu Kα radiation, with a four-circle diffractometer and HiStar multiwire area detector. ^{13}C NMR spectra were recorded on a Varian Mercury 400 spectrometer operating at 100.6 MHz. FTIR spectra were measured on a Galaxy Series FTIR 5000 spectrometer by means of KBr pellets.

3. Results and discussion

3.1. Synthesis and morphology of PNT

CTFMP and CTFSP were used to simultaneously polymerize and crystallize PNT crystals. The polymer thin films polymerized through these techniques are thin enough for observation in a TEM.

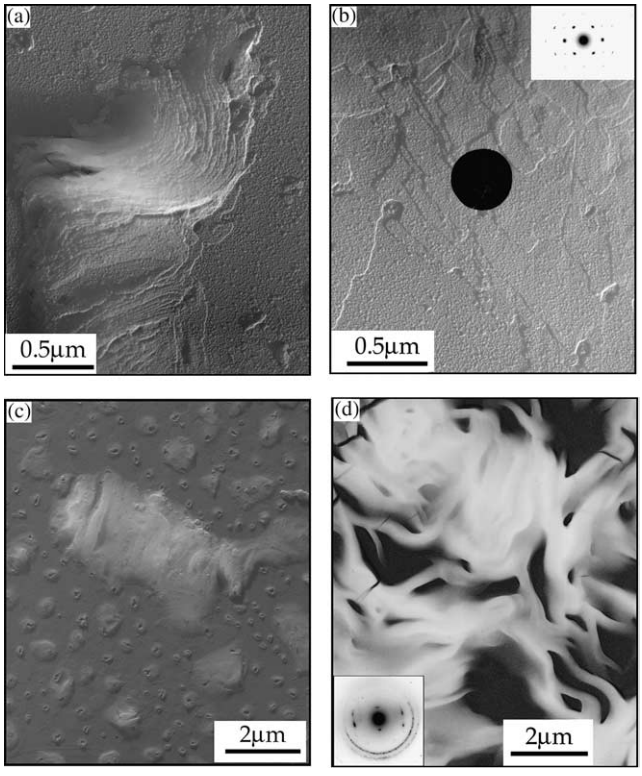

Fig. 1. TEM micrographs of PNT prepared by CTFMP: (a), (b) 170/2, glass, (c) 170/24, and (d) 230/4.5, mica.

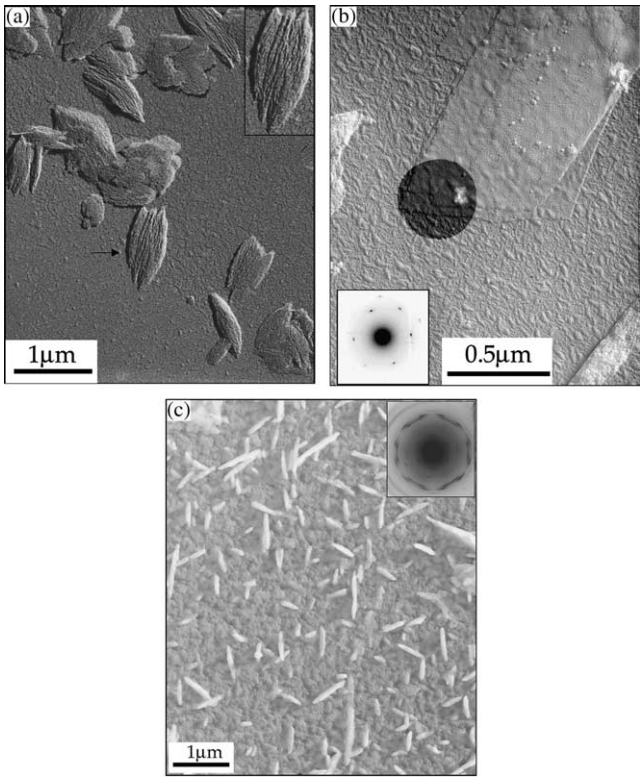

Fig. 2. TEM micrographs of PNT prepared by CTFSP in Therminol 66: (a) 350/46, glass, (b) TC/2,6-DAN, 300/6, mica, and (c) 350/17, mica.

CTFMP was carried out at various temperatures. Polymerization at lower temperatures usually results in well-defined lamellar structures. Fig. 1(a) and (b) are the typical morphology of CTFMP sample polymerized between glass cover slips at 170 °C for 2 h. Both lamellae (ca. 70 Å thickness) on edge (Fig. 1(a)) and lamellae (ca. 50–100 Å thickness) parallel to the substrate (Fig. 1(b)) were observed.

The lamellae parallel to the substrate (Fig. 1(b)) gave rise to [001] zone patterns with the *c*-axis normal to the lamellae, i.e. the substrate. No ED patterns were obtained from the tilted lamellae (Fig. 1(a)). When polymerization time increases to 24 h, the lamellae seem to merge to form thick structures (Fig. 1(c)). Of particular importance for crystal structure determination was the result of CTFMP between mica. Fig. 1(d) shows the morphology of samples polymerized between mica at 230 °C for 4.5 h. Lamellae on edge with irregular shape and orientation were observed. The inset is a [120] zone pattern from a similar area to that shown in Fig. 1(d).

PNT samples were also prepared by CTFSP. When polymerized between glass cover slips (Fig. 2(a)), small mounds with nearly perpendicular lamellae (see the inset) were observed. No ED patterns were obtained from these perpendicular lamellae. Hoping to obtain epitaxial growth, CTFSP was carried out between mica. Somewhat surprising, epitaxial growth was not seen from TC + 2,6-DAN samples polymerized at 300 °C for 6 h between mica, which instead was

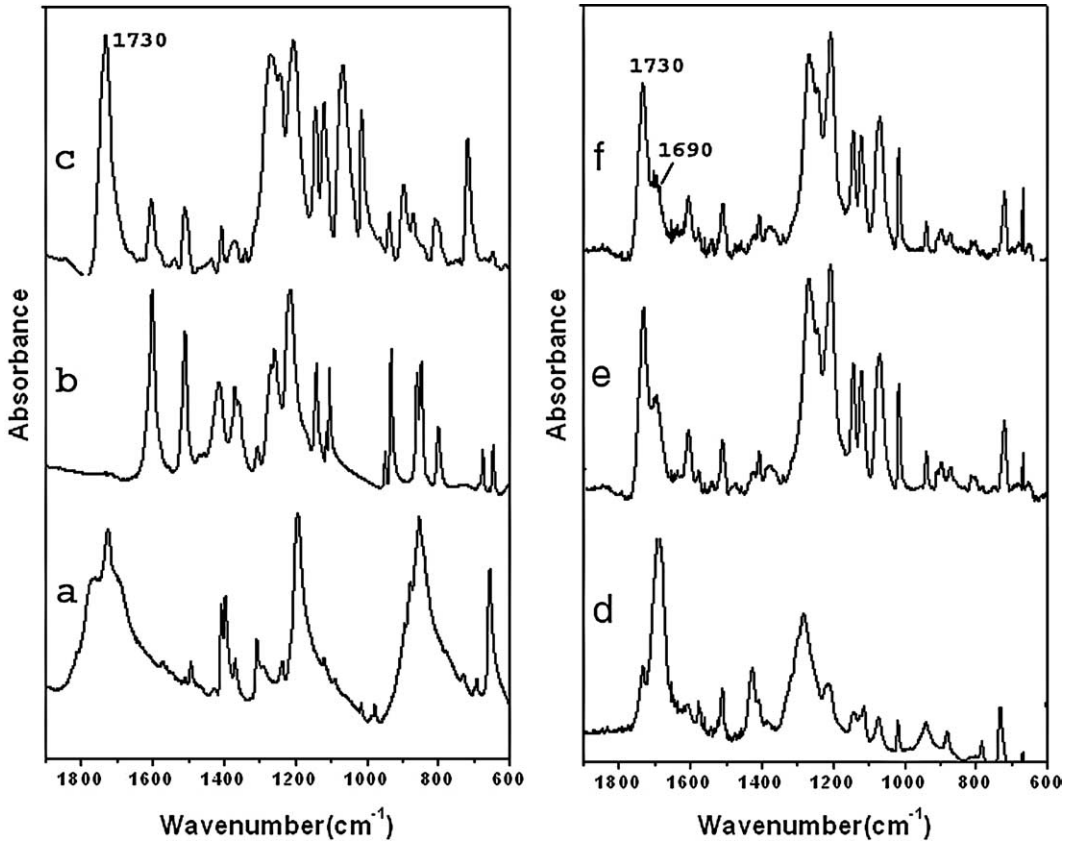

Fig. 3. FTIR spectra (KBr pellets): (a) monomer TC, (b) monomer 2,6-DHN, (c) PNT, 4% (w/v) in Marlotherm SH, 400/5, (d) PNT, CTFMP, 170/2, scraped from substrates, (e) PNT, CTFMP, 170/6, scraped from substrates, (f) PNT, CTFMP, 170/24, scraped from substrates.

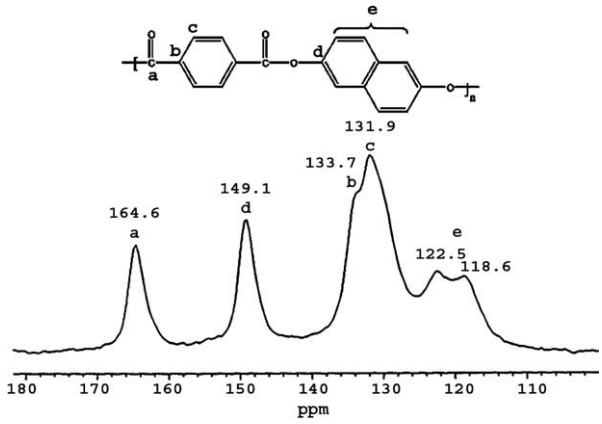

Fig. 4. Solid-state ^{13}C NMR of PNT: 4% (w/v) in Marlotherm SH, 400/5.

composed of ca. 65 Å thick, well-defined lamellae (Fig. 2(b)) lying on the substrate and giving rise to [001] zone patterns (see the inset). However, when CTFSP was carried out with TC + 2,6-DHN between mica at 350 °C for 17 h, epitaxial, thick, on-edge lamellae oriented in three directions at 60° relative to one another developed (Fig. 2(c)). The inset diffraction pattern, from another area, shows the superposition of three [120] + [1$\bar{2}$0] twin patterns oriented at 60° relative to each other.

Besides CTFMP and CTFSP, solution and bulk polymerizations were carried out at relatively high temperatures to obtain powder samples. Since, PNT is insoluble in all common solvents, only a few methods are available for its characterization. Powder samples from solution polymerization and CTFMP samples scraped from substrates were examined using FTIR to verify the esterification reaction and estimate the molecular weight. Fig. 3 is the IR spectra of the two monomers (curves a and b), PNT solution polymerized powder (curve c) and CTFMP samples polymerized at 170 °C for 2, 6 and 24 h, respectively (curves d–f). After polymerization, the characteristic CO bands of terephthaloyl chloride at 1764 and 1694 cm^{-1} (curve a in Fig. 3) disappeared and the peak at 1730 cm^{-1} was replaced by a peak at the same position attributed to ester CO (curves c–f in Fig. 3). For the CTFMP samples the peaks at about 1690 cm^{-1}, due to the CO in the COOH end groups, decrease as the polymerization time increases, while the ester peak at 1730 cm^{-1} increases, suggesting increasing molecular weight. This result agrees with the morphology observation (Fig. 1(a)–(c)). No effort was made to quantitatively determine the molecular weight. No end groups were detected when the polymerization was conducted at 400 °C for 5 h at a 4% concentration in Marlotherm® SH, suggesting a high molecular weight for the high temperature, solution polymerized sample (curve c in Fig. 3). The solid state ^{13}C NMR spectrum of the same solution polymerized powder sample as in Fig. 3(c) confirmed the structure of PNT (Fig. 4); no end groups were detected.

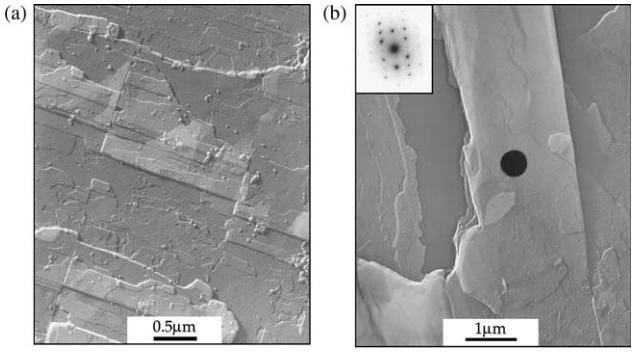

Fig. 5. TEM micrographs of PNN CTFMP samples of NDADME/DAN polymerized at 250 °C for 16 h between glass slides. The inset ED pattern is from the highlighted area and is properly oriented relative to the crystal.

3.2. Synthesis and morphology of PNN

One difficulty in the application of CTFMP in the preparation of PNN is that one of the commercially available monomers, 2,6-NDADME, does not dissolve in acetone or other low boiling point solvents. Thus powder mixtures of the two monomers were used in the polymerization; the large amount of materials in the polymerization results in thick crystals, often spanning the gap between the substrates. Fig. 5 shows pictures of the typical morphology. Split, thick, stacks of lamellae are present; the individual lamellae are on the order of 90–110 Å thick. The inset in Fig. 5(b) is the ED from the highlighted area and is properly oriented.

3.3. Electron diffraction results for PNT

Electron diffraction patterns from various zones are shown in Fig. 6. The variation of intensity distribution in the [001] zone has been extensively discussed in the work for PPN [13] and PPT [12]. Similar intensity variation in [001] zone patterns

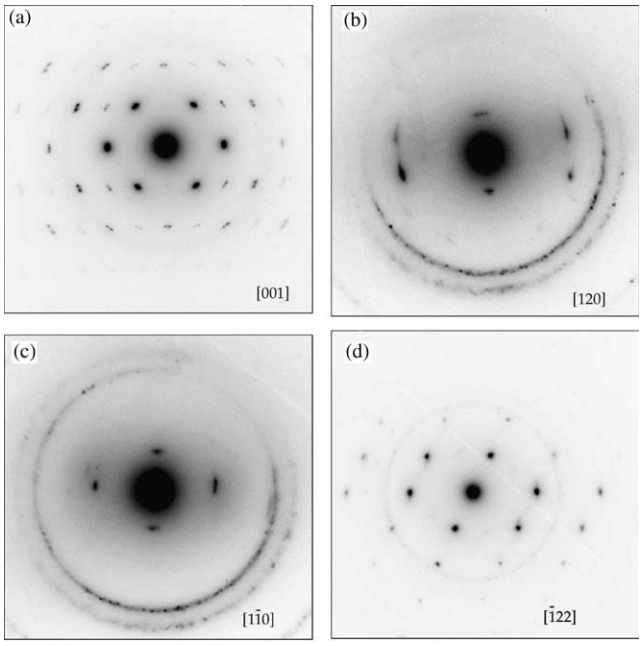

Fig. 6. ED patterns of PNT from various zones: (a) [001], 170/2, glass, (b) [120], 230/4.5, mica, (c) (1$\bar{1}$0), 230/4.5, mica, and (d) [$\bar{1}$22], obtained by shearing oligomers shortly after heating started, then continuing polymerization at 170 °C for 2 h.

Table 1
Spacings of PNT from ED and XRD

Reflections	Spacings (Å)					
	Observed ED				Simulated ED	XRD
	[001]	[120]	[$\bar{1}$22]	Fiber		
200	4.02[a]			4.04	4.00	4.04
110	4.68[a]			4.68	4.70	4.63
210	3.31[a]	3.31	3.25		3.29	3.30
310	2.40[a]				2.42	
020	2.92[a]				2.90	
211		3.13[a]			3.10	3.10
002		7.30[a]		7.48	7.29	
0$\bar{1}$1			5.18		5.39	5.25

[a] Spacings from these reflections were used in the unit cell refinement.

was observed for PNT. Fig. 6(a) is a typical, presumably untilted, [001] zone pattern obtained by CTFMP between glass at 170 °C for 2 h. Spacing measurement and unit cell packing simulation were based on the [001] zone similar to the pattern shown in Fig. 6(a) with alternating intensity along both a^* and b^*.

Fig. 6(b) and (c) are patterns from zone [120] and zone [1$\bar{1}$0] obtained from a CTFMP sample: 230 °C/4.5 h, between mica. The indices of the reflections can be determined from the corresponding simulation in Fig. 11. The spacings from the [120] zone as well as those from the [001] zone (Table 1) were used in the unit cell parameter refinement. Fig. 6(d) was obtained by shearing the oligomers shortly after heating started, then continuing the polymerization at 170 °C for 2 h. The spacings from this zone, [$\bar{1}$22], are shorter than the corresponding ones from other zones and those from simulation (Table 1). This is probably due to a defective structure resulted from the shearing.

ED patterns from the CTFSP epitaxial samples are shown in Fig. 7(a) and (b). Fig. 7(a) is a twinned pattern. Fig. 7(b) consists of three patterns similar to the pattern in Fig. 7(a), at 60° to each other. The inset clearly shows the three

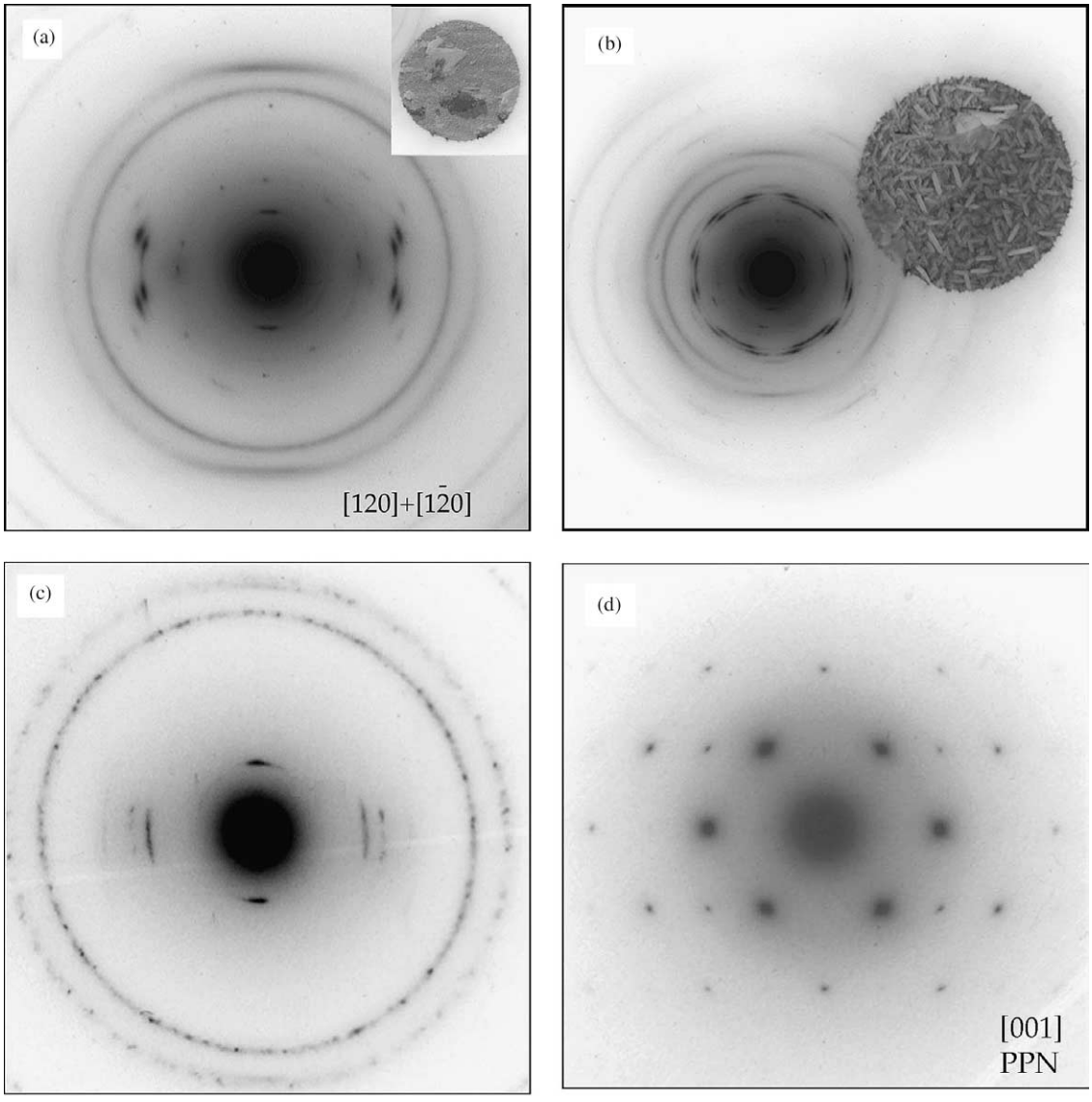

Fig. 7. ED patterns of PNT: (a), (b) epitaxial samples, 1% Therminol 66, 350/17, mica, and (c) fiber, resulted from shearing the CTFMP sample (170/6, glass) at 350 °C, and (d) [001] ED pattern of PPN for comparison purposes.

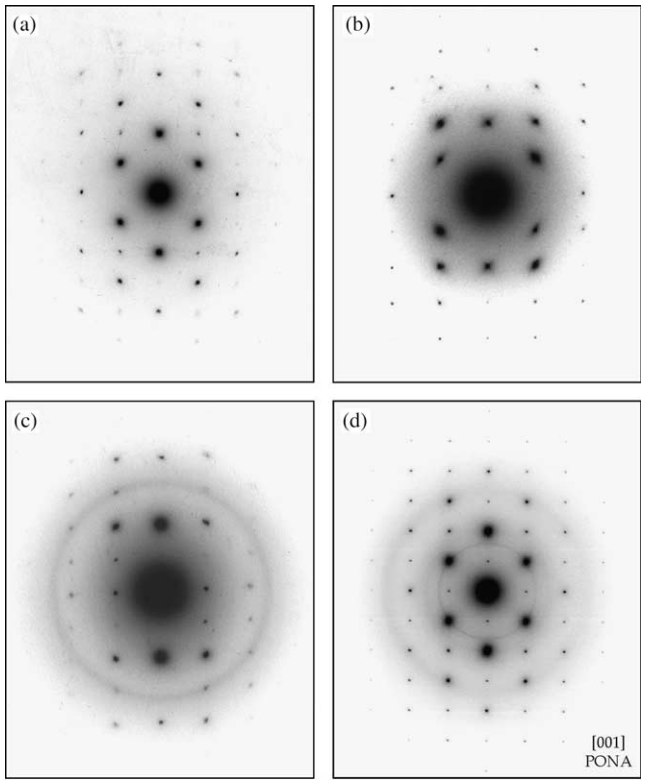

Fig. 8. ED patterns of PNN CTFMP samples from NDADME/DAN at 250 °C for 16 h between glass slides. (a) Typical [001]; (b) [001] tilted about b; (c) [011]; (d) [001] ED pattern of phase I PONA for comparison.

orientations. The spacings from these two CTFSP epitaxial samples agree with those from CTFMP between mica.

A fiber pattern obtained by shearing a CTFMP sample (170 °C/2 h, glass) at 350 °C is shown in Fig. 7(c). It has only a few reflections, including (002), (110) and (200), indicating relatively imperfect crystals. Also shown, in Fig. 7(d), is an [001] ED pattern from PPN polymerized from 2,6-naphthaloyl dichloride and hydroquinone (250 °C/16 h, glass) for comparison purposes (see below) with the [001] pattern for PNT in Fig. 6(a).

3.4. Electron diffraction results of PNN

Fig. 8(a) is a typical [001] zone pattern. It is a good pattern in terms of number of reflections and symmetry. In this pattern, the (200) and (110) are strong and the intensity alternates along both the a^* and b^* axis. For example, (310) is stronger than (210). Fig. 8(b) is also from [001] zone but the crystal is slightly tilted about the b-axis resulting in (210) being stronger than (310). Fig. 8(c) is from the [011] zone, obtained by tilting the specimen. Polymerization between mica did not give epitaxial growth, as compared with PONA [16].

The patterns in Fig. 8(a) and (c) were used in the unit cell parameter refinement, with the spacings listed in Table 3. The parameters after refinement are: $a=7.85$, $b=5.97$, $c=17.1$, $\alpha=90°$, $\beta=99.5°$, and $\gamma=90°$.

For comparison, a typical [001] pattern of phase I PONA is shown in Fig. 8(d). In PONA phase I pattern, all $hk0$ reflections

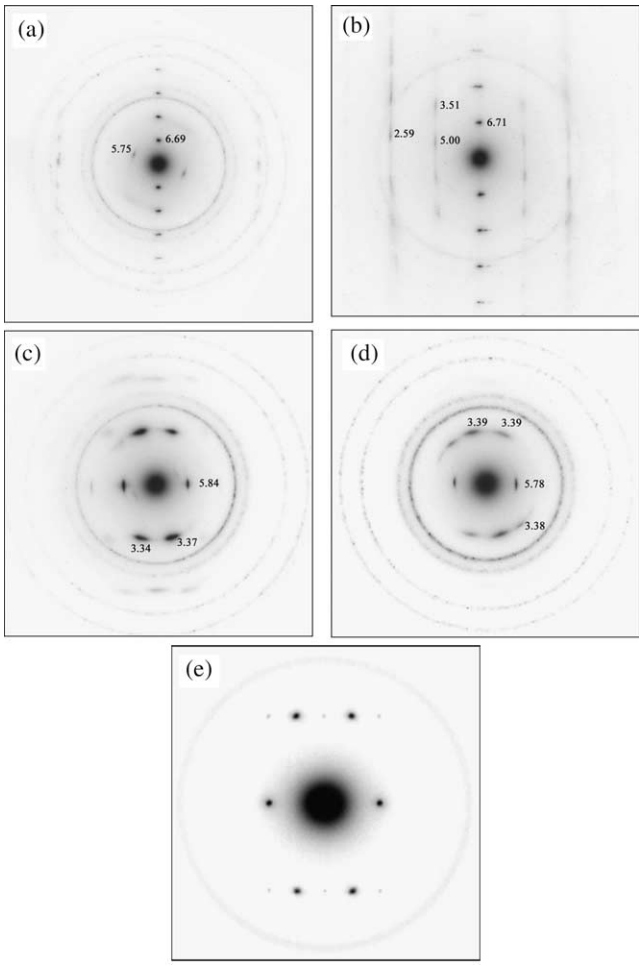

Fig. 9. ED patterns of PNN CTFSP samples from NDADME/DAN at 350 °C for 23 h between glass slides (a)–(c), and mica (d); decorated with gold for inner calibration. For comparison, an [001] ED pattern of phase II PONA (180 °C/4 h) is shown in (e).

are present, with $h+k$ odd weaker than $h+k$ even, while for PNN, most $h+k$ odd reflections are completely absent.

Fig. 9 shows ED patterns from CTFSP with 1% monomers in Marlotherm at 350 °C for 23 h. The spacings from these patterns do not match any of the reflections shown in Fig. 8 (compare with Table 3). These ED patterns may be due to phase II PNN structure, with a second phase having been observed for PONA (Fig. 9(e)) [8], and P*p*OBA [17,18]. There are not enough patterns to determine the crystal structure of phase II PNN.

3.5. PNT crystal structure

Refinement of the unit cell parameters, using the spacings from [001] and [120] zone patterns (Table 1) resulted in values of $a=8.18$ Å, $b=5.80$ Å, $c=14.9$ Å and $\beta=101.9°$. With space group $P12_1/a1$, a unit cell was proposed using Cerius[2]. The three projections perpendicular to a, b and c-axes are shown in Fig. 10. For comparison, the three corresponding projections of poly(*p*-phenylene 2,6-naphthalate) [13] are also shown in Fig. 10.

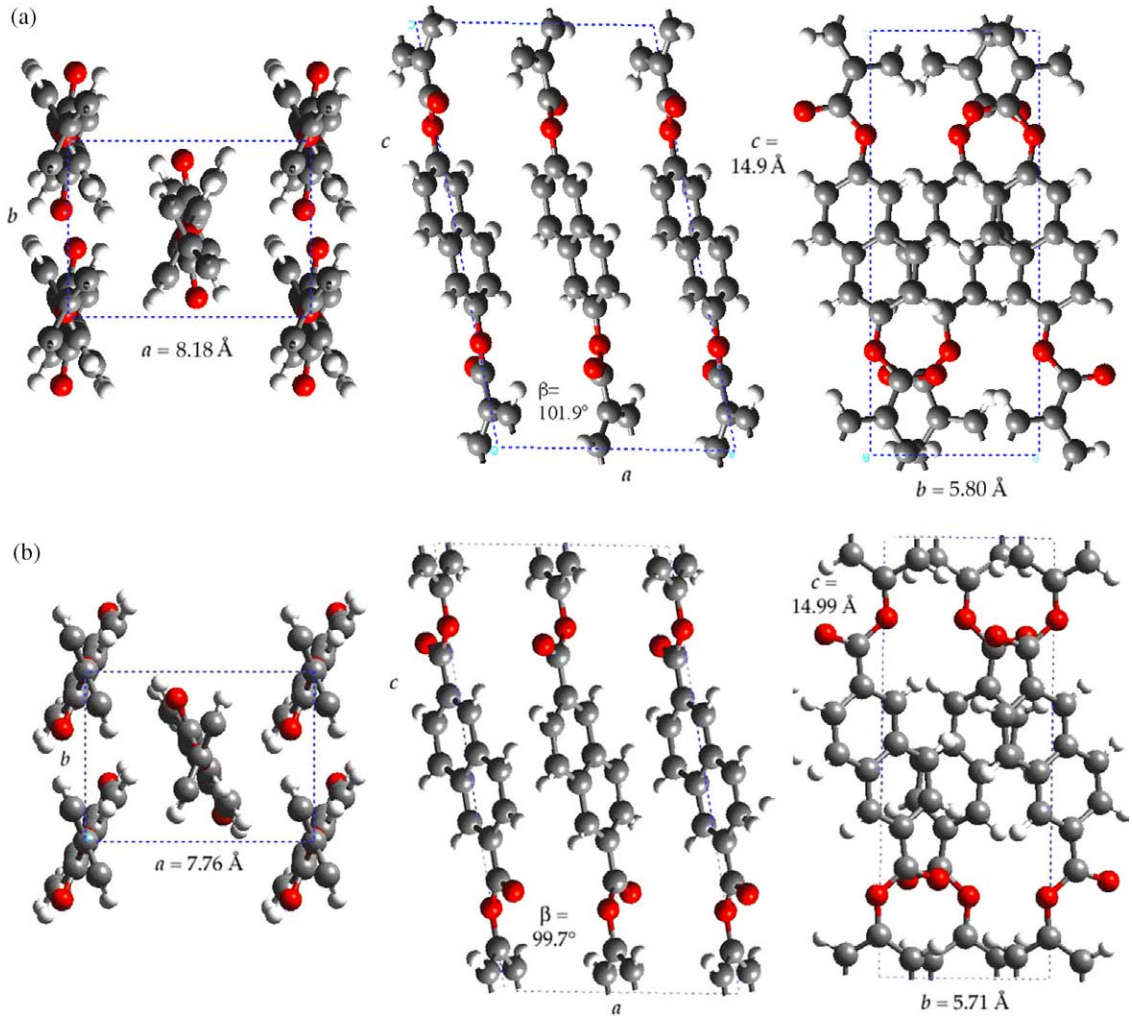

Fig. 10. Three projections of the simulated unit cells: (a) PNT, $a=8.18$ Å, $b=5.80$ Å, $c=14.9$ Å and $\beta=101.9°$, space group $P12_1/a1$, and (b) PPN, $a=7.76$ Å, $b=5.71$ Å, $c=14.99$ Å and $\beta=99.7°$, space group $P12_1/a1$ [13].

The cell parameters of these two polymers are similar with a slightly larger a, b, β and a smaller c for PNT (Fig. 10). The experimental uncertainty of the unit cell parameters from the ED spacing measurements and unit cell refinement program should be less than 0.05 Å. So the observed differences (0.09 Å in b and c, and particularly 0.42 Å in a) are beyond the experimental uncertainty. The [001] projection of these two unit cells after energy minimization shows that the biggest difference in packing is that for PNT the carbonyl group forms an angle to both the phenylene and naphthalene ring, while for PPN the carbonyl group is parallel to the naphthalene ring.

Various zone ED patterns, simulated based on the proposed PNT unit cell (Fig. 10), are shown in Fig. 11. These simulated patterns are all in good agreement with the observed patterns (Fig. 6). For example, the intensity alternates on the row line in the [001] zone and the intensity of the $(\bar{2}11)$ reflection is stronger than that of (211) in the [120] zone. The only obvious discrepancy is that for the $[\bar{1}22]$ zone, the observed spacings are shorter than simulated values. As stated before, the $[\bar{1}22]$ zone was obtained by shearing the oligomers. The shearing might result in a defective structure and account for the shorter spacings even though the reflections are all relatively sharp. Shearing often causes defective crystal structures. For example, significant differences (both positions and intensities) between the experimental fiber patterns obtained by shearing and the calculated fiber patterns based on perfect single crystals was found for PET [2].

The (002) spacing of PNT fiber is also significantly different from that of unsheared single crystals (see Table 1).

A comparison of the calculated $hk0$ intensities for PNT and PPN is given in Table 2, relative to the intensity of (200) for both polymers. As indicated, (110), (310) and (220) appear relatively stronger in the [001] ED pattern of PPN (Fig. 7(d), similar to Fig. 6(a), [13]) than for PNT (Fig. 5(a)) while (400) is weaker, all in agreement with the simulated values. The strong (400) in PNT is attributed to the oxygen atoms lying on planes with a 1/4 b spacing while the projected density parallel to the 310 planes is higher in PPN. Only (420) appears to be weaker than simulated in the PPN pattern, being weaker in the pattern than a number of other reflections that have weaker simulated values.

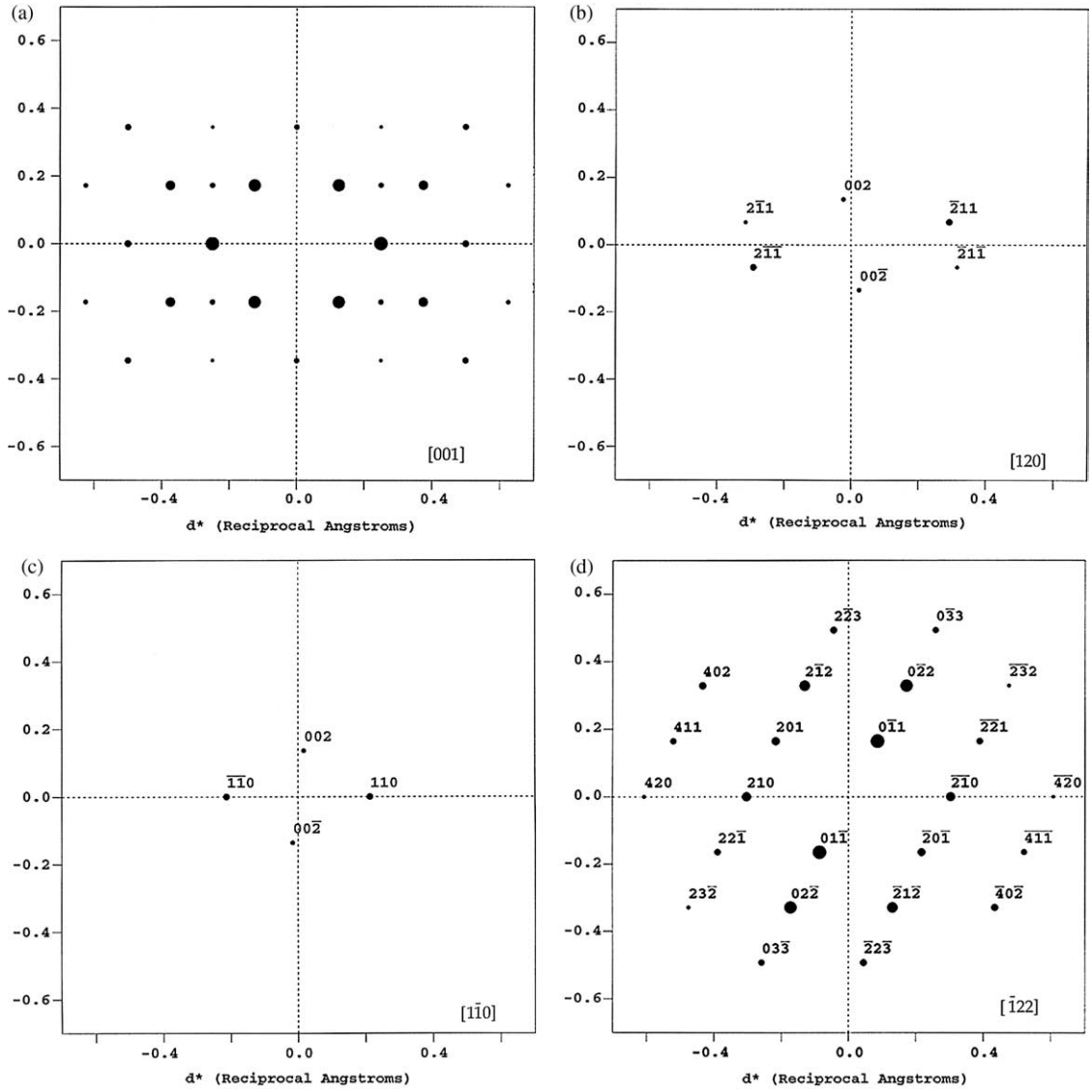

Fig. 11. Simulated ED patterns of PNT based on unit cell in Fig. 7: (a) [001], (b) [120], (c) [1$\bar{1}$0] and (d) [$\bar{1}$22]. The patterns were simulated with crystal thickness and intensity of 50 Å, 5 for (a), 150 Å, 0.5 for (b) and (c), and 100 Å, 50 for (d).

A WAXS scan of bulk polymerized PNT powder (350/25.5) is shown in Fig. 12 with the main peaks indexed. The number of reflections observed is smaller than from ED. The spacings from WAXS are similar to those from ED (Table 1), except for a smaller (0$\bar{1}$1) compared to simulated ED values. The (0$\bar{1}$1)

Table 2
Comparison of simulated [001] zone intensity for PNT, PPN, PNN and PONA (15)

hkl	Intensity (%)			
	PNT	PPN	PNN	PONA
200	100.00	100.00	100.00	100.00
110	31.34	51.65	25.50	36.96
310	11.49	23.65	19.79	14.63
400	3.10	0.39	1.48	0.10
420	2.14	4.30	5.08	1.37
020	1.25	1.74	1.14	0.32
210	1.21	1.34	0.36	11.00
220	0.23	1.41	0.43	0.29

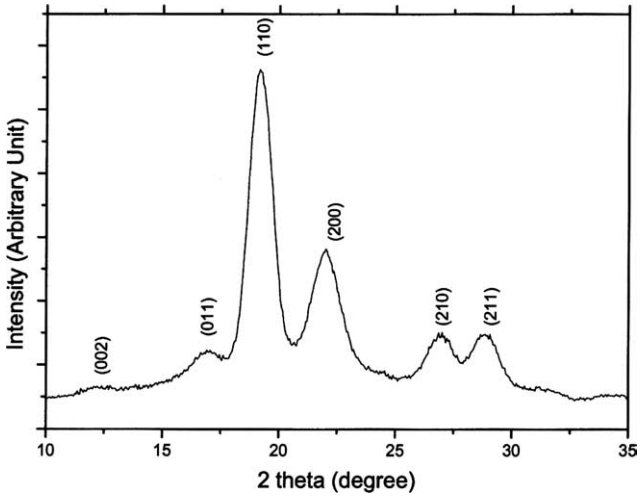

Fig. 12. WAXS of PNT powder: bulk polymerization, 350/25.5.

Table 3
ED spacings of PNN and PONA

Reflections	ED Spacings (Å)		Simulated Å	Simulated Å (PONA)
	[001]	[011]		
200	3.90[a]	3.83	3.87	3.83
400	1.90[a]	1.93	1.94	1.91
110	4.74[a]		4.72	4.67
210	3.23[a]		3.24	3.21
020	2.96[a]		2.98	2.95
011		5.55[a]	5.61	5.58
211		3.09[a]	3.11	3.09

[a] Spacings from these reflections were used in the unit cell refinement.

peak in WAXS is small and broad, which can cause the difficulty of measuring the spacing. Unfortunately, the 002 reflection is also too broad and weak to permit a reliable measurement to compare with the two ED spacings (Table 3).

3.6. PNN crystal structure

The proposed phase I crystal structure of PNN is shown in Fig. 13. It is monoclinic with space group $P12_1/a1$. As in PNT, which it resembles in all projections, there are two molecules in the cell, one in the center and the other in the corner. The two chains are parallel to the *c*-axis direction with the ester group in

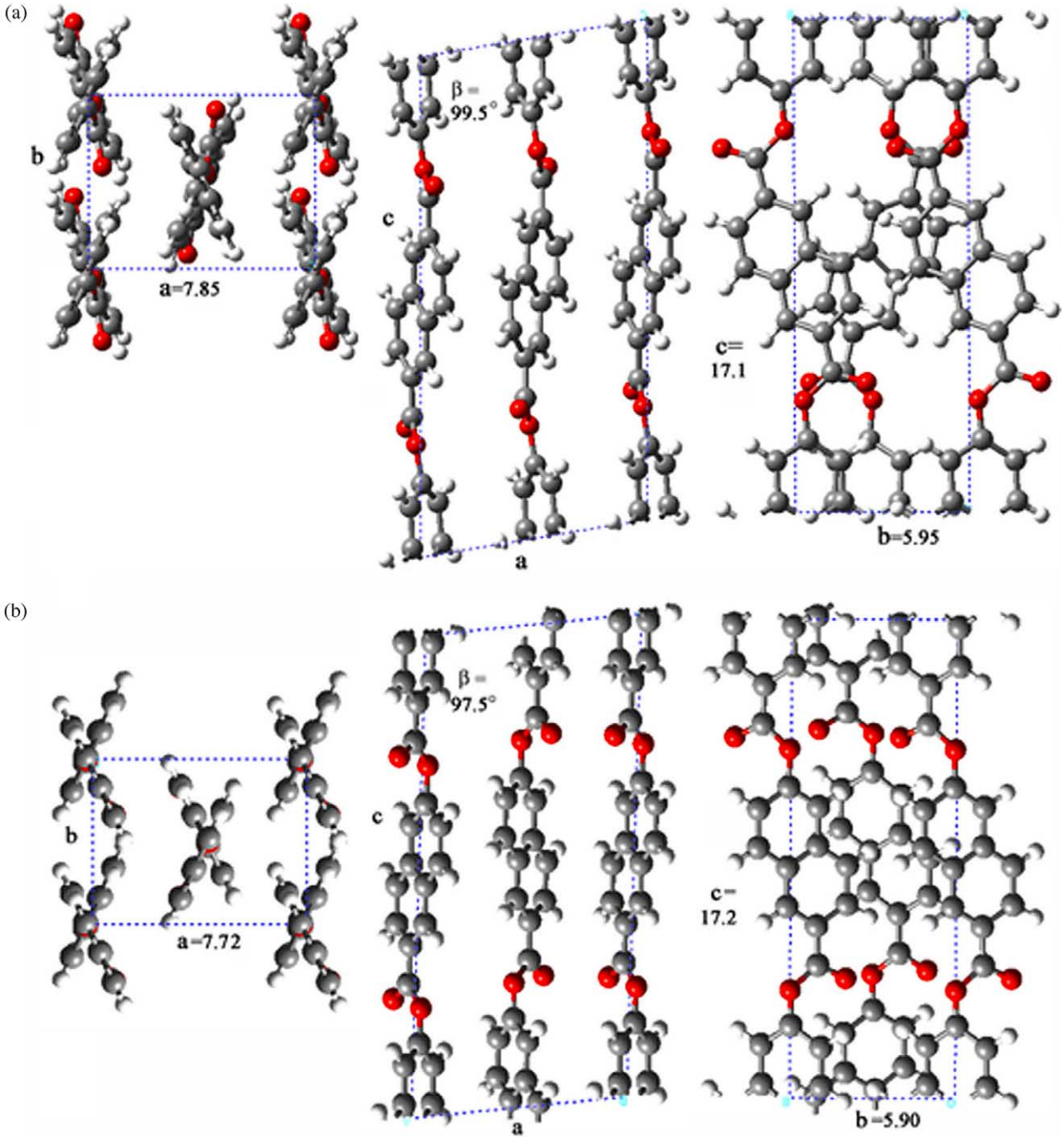

Fig. 13. Three projections of the simulated unit cells: (a) PNN, $a=7.85$ Å, $b=5.94$ Å, $c=17.1$ Å, $\beta=99.5°$, space group $P12_1/a1$, and (b) PONA, $a=7.72$ Å, $b=5.90$ Å, $c=17.2$ Å and $\beta=97.5°$, space group $P1$ [15].

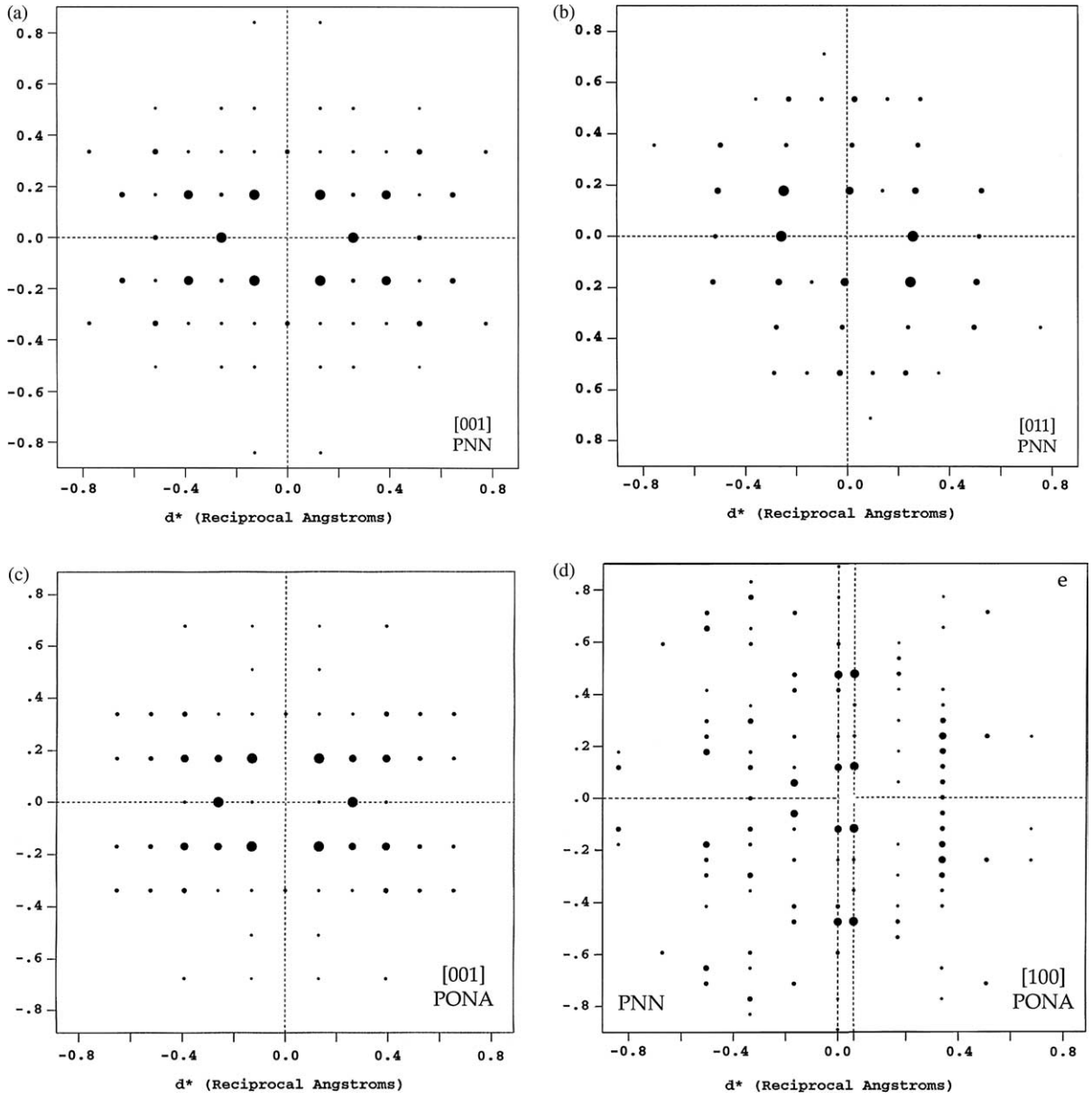

Fig. 14. Comparison of simulated (a [001], b [011] and d [100]) ED patterns of PNN and PONA (c [001] and e [100]).

the same plane as the naphthalate ring. For comparison, the three corresponding projections of poly(2,6-oxynaphtalate) (PONA) [13] are also shown in Fig. 13. The primary difference is in the [100] projection, successive chemical repeat units in PNN (and PNT and PPN, Fig. 10) tilting in opposite directions at the corners and in the middle of the unit cell, whereas for PONA they tilt in the same direction. In addition, in the [001] projection the four arms of the 'cross' are of more equal length, although the carbonyl groups lie along only one of the arms.

The simulated ED patterns for [001] and [011] zones are shown in Fig. 14. For the [001] zone, the simulated patterns agree very well with the experimental ones. However, for the [011] zone, there is a discrepancy in intensity. In the simulated pattern, the $(1\bar{1}1)$ and $(\bar{1}1\bar{1})$ are visible and $(\bar{1}\bar{1}1)$ and $(11\bar{1})$ are absent; while in the experimental pattern, it is the opposite: $(1\bar{1}1)$ and $(\bar{1}1\bar{1})$ are absent but $(\bar{1}\bar{1}1)$ and $(11\bar{1})$ are visible. One explanation is that the experimental pattern is slightly tilted from the [011] zone, so the apparent $(\bar{1}11)$ and $(1\bar{1}1)$ are actually residual reflections from the [001] zone. To confirm the unit cell additional zone patterns, for instance from epitaxial growth, are needed. However, we have been unable to obtain epitaxial growth by CTFMP or CTFSP between mica so far. Also shown are simulated patterns for [001] PONA and [100] for PNN and PONA. Table 2 lists the simulated *hk*0 intensities for PNN and PONA, in addition to PNT and PPN. Comparing the [001] simulated patterns, as in the ED patterns (Fig. 8(a) and (d)), PNN has a greater alternation in intensity along the *h*10 row than PONA and 420 is strong for PNN while 320 is strong for PONA in the *h*20 row of reflections, a difference we attribute to the differences in alignment of the carbonyl groups in the [001] unit cell projections in Fig. 13. As expected, due to the significantly different projections of the

unit cell electron density, a much larger difference in the simulated patterns is seen for the [100] patterns. The [010] zones also differ (not shown) in that PONA [010] has *hkl* row lines with *h* odd and even while PNN has them only for *h* even and PNN has *hkl* row lines with *k* odd and even but PONA has them only for *k* even; we attribute the latter difference to the difference in ester group orientations; while the former would be due to the central molecular segment having a different projection than those at the corners. Unfortunately, as indicated, we were unable to obtain PNN ED patterns containing the c^*-axis although [100] and [010] were obtained for PONA in good agreement with the simulations [13].

4. Conclusions

Poly(2,6-naphthalene terephthalate) was synthesized from TC and 2,6-DHN or 2,6-DAN by solution polymerization, bulk polymerization and confined thin film melt/solution polymerization. The chemical structure of PNT was confirmed by FTIR and ^{13}C NMR. Epitaxial growth was observed from CTFSP between mica. The crystal structure of PNT was determined by examination of the electron diffraction from the thin film samples, combined with the molecular modeling. The obtained unit cell parameters are similar to those of PPN. A unit cell packing was proposed based on the cell parameters obtained from ED and space group $P12_1/a1$. The simulated patterns agree fairly well with the observed patterns, suggesting the correctness of the proposed unit cell.

The morphology of poly(2,6-naphthalene 2,6-naphthalate), prepared by confined thin film melt polymerization (CTFMP) using 2,6-NDADME and 2,6-DAN, was characterized by TEM. Split thick crystals were observed. Besides [001] zone ED patterns, [011] zone ED patterns were obtained by tilting the specimen and used in the unit cell refinement. No epitaxial growth was obtained by CTFMP or CTFSP between mica. Crystal structure was simulated with Cerius^2. A unit cell was proposed with $a=7.85$, $b=5.97$, $c=17.1$ Å, $\beta=99.5$, and space group $P12_1/a1$. Simulated ED patterns agree reasonably well with experimental patterns. The ED patterns observed from CTFSP samples polymerized at high temperature are probably due to phase II PNN.

Acknowledgements

This research was supported, in part, by Grant DMR 0234678 from the Polymer and International Programs sections of the U.S. National Science Foundation and Grant ME-131 from the Granting Agency of the Czech Republic. The majority of the TEM was carried out in the Center for Microanalysis of Materials, University of Illinois, which is partially supported by the U.S. Department of Energy under grant DEFG02-91-ER45439.

References

[1] Liu J, Geil PH. J Macromol Sci, Phys 1997;36(2):263–80.
[2] Liu J, Geil PH. J Macromol Sci, Phys 1997;36(1):61–85.
[3] Liu J, Yuan B-L, Geil PH, Dorset DL. Polymer 1997;38(24):6031–47.
[4] Rybnikar F, Geil PH. J Polym Sci, Part B: Polym Phys 1997;35(11):1807–20.
[5] Yuan B-L, Rybnikar F, Saha P, Geil PH. J Polym Sci, Part B: Polym Phys 1999;37(24):3532–51.
[6] Rybnikar F, Saha P, Yuan B-L, Geil PH. J Polym Sci, Part B: Polym Phys 1999;37(24):3520–31.
[7] Rybnikar F, Liu J, Myers JA, Geil PH. Korea Polym J 1998;6(1):53–74.
[8] Liu J, Rybnikar F, Geil PH. Korea Polym J 1998;6(1):75–83.
[9] Liu J, Sidoti G, Hommema JA, Geil PH, Kim JC, Cakmak M. J Macromol Sci, Phys 1998;37(4):567–86.
[10] Yang J, Sidoti G, Liu J, Geil PH, Li C-Y, Cheng SZ-D. Polymer 2001;42(16):7181–95.
[11] Wang B, Li C-Y, Hanzlicek J, Cheng SZ-D, Geil PH, Grebowicz J, et al. Polymer 2001;42(16):7171–80.
[12] Yang J, Wang J, Sidoti G, Liu J, Rybnikar F, Kaszonyiova M, et al. Chin J Polym Sci 2003;21(2):189–204.
[13] Yang J, Wang J, Sidoti G, Liu J, Rybnikar F, Kaszonyiova M, et al. Chin J Polym Sci 2003;21(2):205–21.
[14] Rybnikar F, Liu J, Geil PH. Macromol Chem Phys 1994;195(1):81–104.
[15] Liu J, Rybnikar F, Geil PH. J Polym Sci Pol Phys 1992;30(13):1469–82.
[16] Schwarz G, Kricheldorf R. Macromolecules 1991;24(10):2829–33.
[17] Hanna S, Windle AH. Polymer 1992;33(13):2825–33.
[18] Iannelli P, Yoon DY, Parrish W. Macromolecules 1994;(27):3295–300.